JOURNAL OF GEOPHYSICAL RESEARCH: ATMOSPHERES, VOL. 118, 9035–9047, doi:10.1002/jgrd.50695, 2013

Uncertainties on the simulated summer precipitation over Eastern China from the CMIP5 models

Dan-Qing Huang,[1] Jian Zhu,[2] Yao-Cun Zhang,[1] and An-Ning Huang[1]

Received 13 April 2013; revised 30 July 2013; accepted 31 July 2013; published 30 August 2013.

[1] Based on 14 climate models from the Coupled Model Intercomparison Project Phase 5 (CMIP5), uncertainty on the simulated summer precipitation over Eastern China is analyzed by investigating the intercomparison between individual model and multimodel ensemble (MME). Generally, MME has the ability in reproducing summer precipitation over Eastern China. However, large model spread exists among models in both climatology and interannual variation. The possible reason for the large model spread lies in the uncertainties on simulating large-scale circulations, e.g., East Asian subtropical westerly jet, western Pacific subtropical high, and East Asian summer monsoon. To investigate uncertainties in different regions, Eastern China is divided to four subregions: South China (SC), Yangtze-Huaihe River Basin (YHRB), North China (NC), and Northeast China (NEC). The annual cycle of regional mean precipitation from 14 CMIP5 models indicates that the model spread approaches maximum in early summer over SC and YHRB and in middle summer over NC and NEC. Uncertainties generally decrease from south to north, with the most sensitive region of SC. For different-class precipitation, the uncertainties of 14 models are small in relatively weak rain, but large in heavy and nonrainfall for all the four regions. We propose two possible reasons for the large uncertainties: different partitioning of stratiform/convective precipitation and horizontal resolutions.

Citation: Huang, D.-Q., J. Zhu, Y.-C. Zhang, and A.-N. Huang (2013), Uncertainties on the simulated summer precipitation over Eastern China from the CMIP5 models, *J. Geophys. Res. Atmos.*, *118*, 9035–9047, doi:10.1002/jgrd.50695.

1. Introduction

[2] Monsoon is defined as a seasonal reversal of the prevailing wind that lasts for several months. Eastern China is dominated by the East Asian summer monsoon (EASM) and is under the influence of the associated rainfall [*Ding and Chan*, 2005]. In summer, Eastern China is vulnerable to floods and droughts due to the relative concentration and severity of the rainfall [*Huang et al*., 2007; *Ye and Lu*, 2012], which accounts for about 70% of the annual rainfall. Therefore, it is worthy to understand the summer rainfall over Eastern China.

[3] The summer rainfall variation has been considered in several studies to evaluate the performance of the climate models [*Meehl et al*., 2007a]. *Huang et al*. [2011] investigated the variation of Baiu system (defined as the severity and duration of summer rainfall affecting China, Japan, Korea, and the surrounding seas) based on the coupled climate model (Miroc_hires3.2) from the University of Tokyo. Results showed that the Miroc_hires3.2 generally captures the three-dimensional structure of the Baiu system. The summer monsoon rainfall in the entire East Asian region is expected to enhance owing to global warming [*Hu et al*., 2000; *Min et al*., 2004; *Lu et al*., 2007]. Although the studies mentioned above show consistent features in multimodels, large uncertainties still exist in climate projections [*Zhou et al*., 2008; *Lau et al*., 2013]. In the same CO_2 doubling experiment, the climate sensitivity in global mean is around 2–5°C in the models from coupled model intercomparison project phase 3 (CMIP3) [*Stephens*, 2005; *Randall et al*., 2007]. On the regional climate change over China, *Chen et al*. [2011] indicated that the Beijing Climate Center (BCC) climate model could capture the predominant spatial patterns of the climatology extreme temperature and extreme precipitation events, but with large systematic bias. *Li and Zhou* [2010] investigated the climate change over China based on the multimodel data sets by CMIP3 and revealed a large spread among the 23 models in the precipitation variation. *Sun and Ding* [2008] evaluated the climate model performance on simulating the summer precipitation and monsoon circulation in East Asia and indicated that the response in same grid point was not consistent in 19 models, suggesting large differences exist among models. Thus, characterizing and quantifying uncertainties in climate change are of fundamental importance not only for the purpose of detection and attribution, but also for strategic approaches to adaptation and mitigation.

[4] In order to study the projections, the technique of multimodel ensemble (MME), defined as the average of

[1]School of Atmospheric Sciences, Nanjing University, Nanjing 210093, China.
[2]State Key Laboratory of Hydrology-Water Resources and Hydraulic Engineering, Hohai University, Nanjing 210098, China.

Corresponding author: D. Huang, School of Atmospheric Sciences, Nanjing University, Nanjing 210093, China. (huangdq@nju.edu.cn)

2169-897X/13/10.1002/jgrd.50695

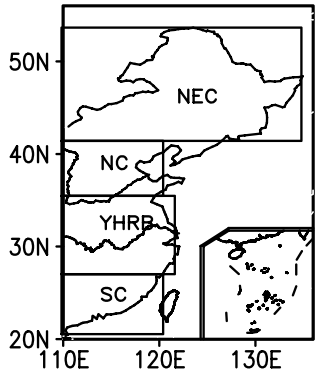

Figure 1. Location of Eastern China and the four subregions. The black boxes indicate the four subregions as South China (SC), Yangtze-Huaihe River Basin (YHRB), North China (NC), and Northeast China (NEC).

simulation results from multiple models has been used. The reason for focusing on MME is that averages across structurally different models empirically show better large-scale agreement with observations [*Cubasch et al*., 2001]. The extensive use of MME in projecting future change therefore provides higher quality and more consistent climate change. The MME has been applied in other models to produce climate features, and therefore improved single models alone [*Christensen et al*., 2007; *Meehl et al*., 2007b]. In future projection, some studies constrained projections using observations, suggesting that the MME performing well in a present-day climate predicts more converged future changes [*Lu et al*., 2007; *Lu and Fu*, 2009; *Jiang et al*., 2012]. However, many aspects of future projections vary widely among different models. It is still unclear that whether utilizing all models for the MME is the best way to obtain more reliable projection [*Knutti*, 2010; *Seo and Ok*, 2013; *Lee and Wang*, 2012]. More realistic outputs can be obtained when the MME is carried out using a suite of well-performing models for a specific variable. This indicates that although an MME is generally better than a single model, the best ensemble mean cannot be achieved without looking into the reliability of individual model, compared with MME [*Sun and Ding*, 2008]. Larger model spread among multimodels indicates larger noises in these models, suggesting less credibility of the MME [*Li and Zhou*, 2010]. Furthermore, a major source of uncertainty in future climate change is model response [e.g., *Hawkins and Sutton*, 2009; *Tebaldi and Knutti*, 2007], which can be the difference between individual models and the MME. Therefore, besides comparing to observations, the intercomparison between individual models and the MME is also important and necessary, especially for estimating the credibility of future projections.

[5] Most recently, climate models from the newest CMIP5, including models with generally higher resolution and a broader set of experiments compared with the CMIP3, have been coordinated to use in the Intergovernmental Panel on Climate Change Fifth Assessment Reports (IPCC AR5) [*Taylor et al*., 2012]. Several studies have used the CMIP5 models for analyzing the future climate change, e.g., the robust decline of subtropical precipitation [*Scheff and Frierson*, 2012], intensification of extratropical cyclones associated with the polar jet [*Mizuta*, 2012], increase of the geopotential height at 500 hPa over Greenland [*Belleflamme et al*., 2012], and expanded westward of land monsoon domain over Asia [*Lee and Wang*, 2012]. Some improvements of the CMIP5 in the skill measures have been reported [*Jones and Carvalho*, 2013; *Hirota and Takayabu*, 2013; *Lee and Wang*, 2012]. However, little attention has been paid to the model uncertainties, especially for the simulated precipitation variation over China. In this study, the following questions are investigated:

[6] 1. How large are the uncertainties on the simulated summer precipitation over Eastern China for 14 CMIP5 models, and where are the most sensitive regions?

[7] 2. What is the possible reason for these uncertainties?

[8] The paper is organized as follows: Data and methodology are described in the next section. Section 3 presents the performance of MME and uncertainties in CMIP5 models, including the climatology, interannual variation, and regional variations and different-class precipitation in summer. Conclusion and discussion are provided in section 4.

Table 1. Models Used in the Study[a]

Model Name	Institute (Country)	Resolution (Atmosphere) (Grids in Longitude) × (Grids in Latitude)
BCC-CSM	Beijing Climate Center, China Meteorological Administration (China)	320 × 160
CanESM2	Canadian Centre for Climate Modeling and Analysis (Canada)	128 × 64
CCSM4	National Center for Atmospheric Research (USA)	288 × 192
CESM1-BGC	Community Earth System Model Contributors (USA)	288 × 192
CMCC-CM	Centro Euro-Mediterraneo per I Cambiamenti Climatici (Italy)	480 × 240
CNRM-CM5	Centre National de Recherches Meteorologiques / Centre Europeen de Recherche et Formation Avancees en Calcul Scientifique (France)	256 × 128
FGOALS-S2	LASG, Institute of Atmospheric Physics, Chinese Academy of Sciences (China)	128 × 108
GFDL-ESM2G	NOAA Geophysical Fluid Dynamics Laboratory (USA)	144 × 90
Inmcm4	Institute for Numerical Mathematics (Russia)	180 × 120
IPSL-CM5A-LR	Institut Pierre-Simon Laplace (France)	96 × 96
MIROC4h	Atmosphere and Ocean Research Institute (The University of Tokyo), National Institute for Environmental Studies, and Japan Agency for Marine-Earth Science and Technology (Japan)	640 × 320
MPI-ESM-LR	Max Planck Institute for Meteorology (Germany)	192 × 96
MRI-CGCM3	Meteorological Research Institute (Japan)	320 × 160
NorESM1-M	Norwegian Climate Centre (Norway)	144 × 96

[a]For all models, the first ensemble member of the historical experiment ("r1i1p1") was analyzed over the period 1979–2005.

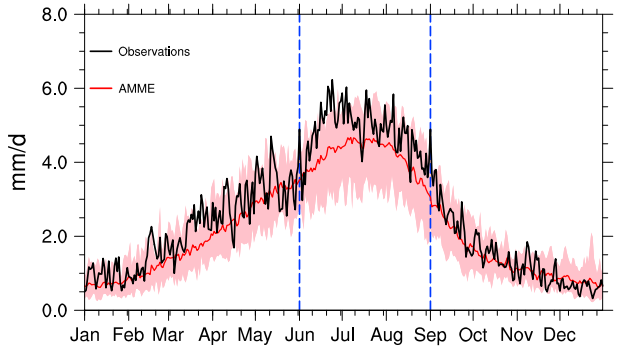

Figure 2. Annual cycle of Eastern-China-averaged daily precipitation from AMME (red solid line), observation (black solid line), and range between maximum and minimum precipitation of the 14 CMIP5 models (pink shading) in 1979–2005. The blue dashed lines indicate summer time. The Eastern-China-averaged precipitation is defined as the area-weighted averaged of two rectangular boxes: (22.5°–43°N, 110°–122.5°E) and (43°–54°N, 110°–130°E). (unit: mm day^{-1}).

2. Data and Methodology

2.1. Data

[9] We examine the precipitation over Eastern China (22.5°–54°N, 110°–130°E, in Figure 1) of historical integrations (forced by observed atmospheric composition changes) from 14 CMIP5 models listed in Table 1, in which the daily precipitation, monthly zonal winds, geopotential height, and cumulus convective precipitation (CCP) from 1979 to 2005 are used. All the model outputs are interpolated onto the horizontal resolution of 1° × 1° using a bilinear interpolation method. To validate the MME, we use the daily precipitation data at 96 meteorological stations in Eastern China during 1979–2005, provided by the China Meteorological Administration.

2.2. Methodology

[10] To investigate uncertainties in different regions, Eastern China is divided into four regions: South China (SC, 22°–27°N, 110°–120°E), Yangtze-Huaihe River Basin (YHRB, 27°–35°N, 110°–122°E), North China (NC, 35°–42°N, 110°–120°E), and Northeast China (NEC, 42°–52°N, 115°–135°E) (boxes shown in Figure 1). Regional time series is calculated as the area-weighted average for each subregion.

[11] Following *Zhou and Yu* [2006], the model spread is used to estimate the uncertainties among models, which is defined as,

$$\mathrm{MS} = \sqrt{\frac{1}{n}\sum_{i=1}^{n}\left(X_i - \overline{X}\right)^2}$$

Where X_i denotes the variable (precipitation, winds, etc.) simulated in individual model, $\overline{X}$ denotes the MME, and n is the ensemble size.

[12] Following *Hirota et al.* [2011], combined two skill scores (R and SDR) defined by *Taylor* [2001], the score (S-index) is used to evaluate the reproducibility of summer precipitation distribution over Eastern China, which is defined as,

$$\mathrm{S} \equiv \frac{(1+\mathrm{R})^4}{4\left(\mathrm{SDR} + \frac{1}{\mathrm{SDR}}\right)^2}$$

Where R is the pattern correlation between the models and the observation and SDR is the ratio of the spatial standard deviations of the models against to that of observations. Thus, S-index quantifies the similarity of the distribution and amplitude of the spatial pattern between the model and the observation.

3. Results

3.1. The Climatological Annual Cycle

[13] Figure 2 shows the annual cycle of All-14-CMIP5-models MME (AMME), observation, and range between maximum and minimum of 14 models for daily precipitation averaged over Eastern China. The AMME shows consistent annual cycle with the observation but underestimates precipitation, especially in summer. It is noteworthy that large uncertainties exist among the 14 CMIP5 models, especially in summer (e.g., the intermodel discrepancy is large). Thus, we focus on summer to investigate the uncertainties on the simulated precipitation over Eastern China.

3.2. Performance of MME in 1979–2005

[14] For seasonal evolution of precipitation over Eastern China, in general, associated with the western Pacific subtropical high (WPSH) jumping northward three times, the EASM advances northward, resulting in the northward movement of the summer rainfall belt. This feature is indicated in the observed latitude-pentad variation of precipitation averaged between 110° and 125°E in Figure 3a. The AMME (Figure 3b)

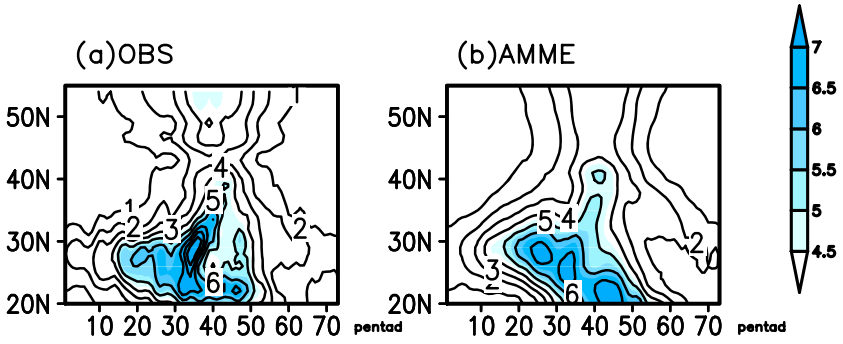

Figure 3. The latitude-temporal sections (110°–125°E) of pentad precipitation for the period of 1979–2005. (a) Observation, (b) AMME. (unit: mm day^{-1}).

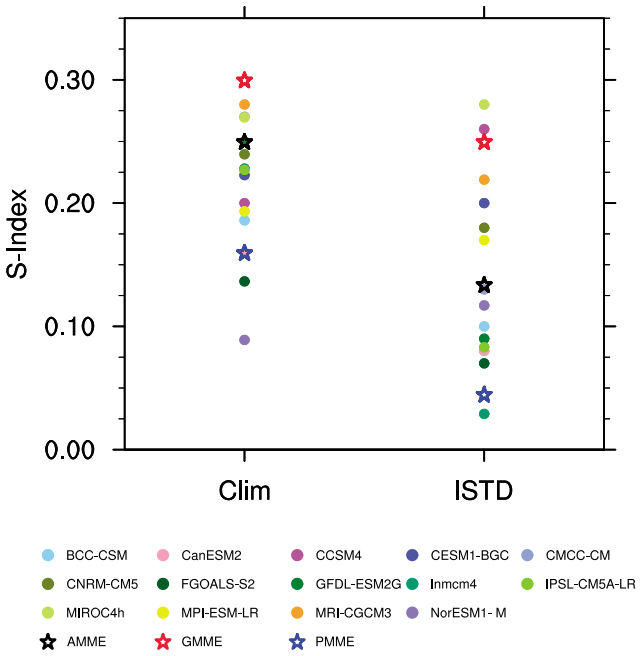

Figure 4. Scores (S-index) of climatology and ISTD of summer precipitation over Eastern China in 1979–2005.

generally captures the simulated monsoon rainfall shift over Eastern China. The simulated rain belt obviously moves northward from early summer, reaches the northernmost around 40th pentad, and later rapidly retreats southward.

[15] For spatial distribution, S-index has been applied recently in the comparison of model performance against observation [*Hirota and Takayabu*, 2013; *Chen et al*., 2013]. In Figure 4, black stars indicate the S-index of AMME is 0.25 and 0.13 for climatology and interannual standard deviation (ISTD), respectively. However, it has been recognized that poorly performing models degrade the overall skill of weather and climate forecasts in an ensemble mean approach [*Krishnamurti et al*., 2000]. Recently, for further assessment of future changes, selecting some best models are needed [*Lee and Wang*, 2012; *Seo and Ok*, 2013]. Thus, it is necessary to check the individual model performance to get better MME performance on simulated precipitation over Eastern China. To select good (highly performing) and poor (poorly performing) models from the 14 CMIP5 models, the S-index of each model is calculated (as solid circles in Figure 4). We refer to models with the five highest and five lowest S-index as good and poor models for climatology and ISTD fields, respectively (Table 2). Calculating the S-index of the good models' MME (GMME) and the poor models' MME (PMME), it shows a significantly increased value of GMME and a largely decreased value of PMME for both climatology and ISTD, compared to AMME (as stars in Figure 4). Furthermore, the spatial distributions of climatology and ISTD are shown in Figure 5 for detailed improvement of GMME. In general, the AMME, GMME, and PMME exhibit a decreasing gradient from south to north, which is quite similar with observation. However, compared to observation (Figures 5a and 5e), the GMME (Figures 5c and 5g) performs better than the AMME (Figures 5b and 5f) and the PMME (Figures 5d and 5h), mainly on the decreased rainfall over northern area and increased rainfall over southeastern area for climatology, and increased interannual variations over southern area for ISTD.

3.3. Uncertainties on Climatology and Interannual Variability

[16] As mentioned above, the GMME performs best on reproducing summer rainfall over Eastern China. However, *Zhou and Yu* [2006] and *Li et al*. [2010] indicated that the model spread was identified as noise among multimodels and reflected the credibility of the MME. Whether the model spread decreases among the good models is still not clear. Figure 6 shows the model spread of all-14, good, and poor models for climatology and ISTD of summer precipitation over Eastern China. As shown in Figures 6b and 6e, good models do not differ much with all-14 models (Figures 6a and 6d) or poor models (Figures 6c and 6f) for model spread in both climatology and ISTD, suggesting that uncertainties or intermodel differences exist among models despite of selecting highly performing models or not. This raises the importance to check the uncertainty in individual model. Additionally, in Figure 6, what common in all-14 models, good models, and poor models are the large model spreads exhibit a decreasing gradient from the south to north for both climatology and ISTD. That indicates that southern China may be the most sensitive region for the summer precipitation simulation.

[17] In order to investigate uncertainty of individual model, we also take MME as a reference following the MS equation described in section 2. Figure 7 shows differences of the spatial distribution of simulated summer precipitation between 14 individual models and the AMME for 1979–2005. The GFDL-ESM2G, MPI-ESM-LR, and FGOALS-S2 models perform more consistently with the AMME than other models. However, large negative biases exist in BCC-CSM, CMCC-CM, and MRI-CGCM3 models, covering most of Eastern China. The CCSM4, CESM1-BGC, and NorESM1-M models show significant positive biases located over the northern part of Eastern China.

[18] Figure 8 compares differences of ISTD of simulated summer precipitation for 1979–2005 between 14 CMIP5

Table 2. The Good and Poor Models Chosen for Climatology and ISTD of Simulated Summer Rainfall Over Eastern China

Climatology		ISTD	
Good Models	**Poor Models**	**Good Models**	**Poor Models**
MRI-CGCM3	NorESM1-M	MIROC4h	Inmcm4
CMCC-CM	FGOALS-S2	CCSM4	FGOALS-S2
MIROC4h	CanESM2	MRI-CGCM3	CanESM2
GFDL-ESM2G	BCC-CSM	CESM1-BGC	IPSL-CM5A-LR
CNRM-CM5	CCSM4	CNRM-CM5	GFDL-ESM2G

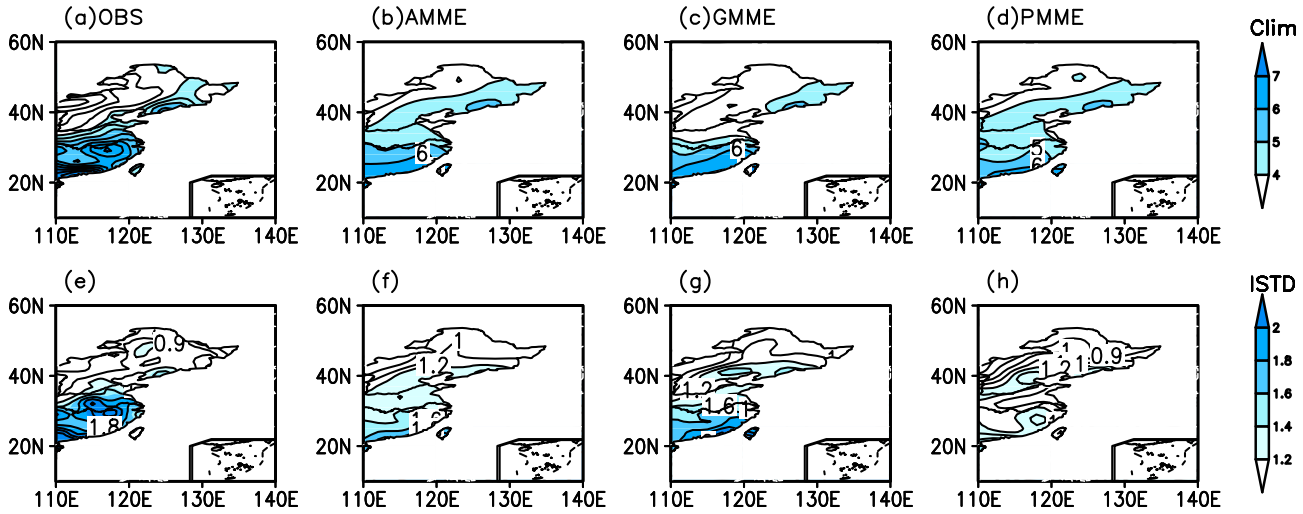

Figure 5. The climatology and ISTD distribution of summer precipitation for the period of 1979–2005. (a,e) Observations, (b,f) AMME, (c,g) GMME, and (d,f) PMME. (unit: mm day^{-1}).

models and the AMME. The MPI-ESM-LR, FGOALS-S2, and CNRM-CM5 models perform closer to the AMME. However, in the southern part of Eastern China, CCSM4, CESM1-BGC, and MIROC4h models show positive biases, while CanESM2, Inmcm4, and IPSL-CM5A-LR models indicate negative biases.

[19] As mentioned above, large uncertainties on the simulated precipitation exist in 14 CMIP5 models. What are the possible reasons for the large uncertainties? As well known, the summer rainfall over Eastern China is associated with large-scale atmospheric circulations, e.g., WPSH and the East Asian subtropical westerly jet (EASWJ) [*Akiyama*,

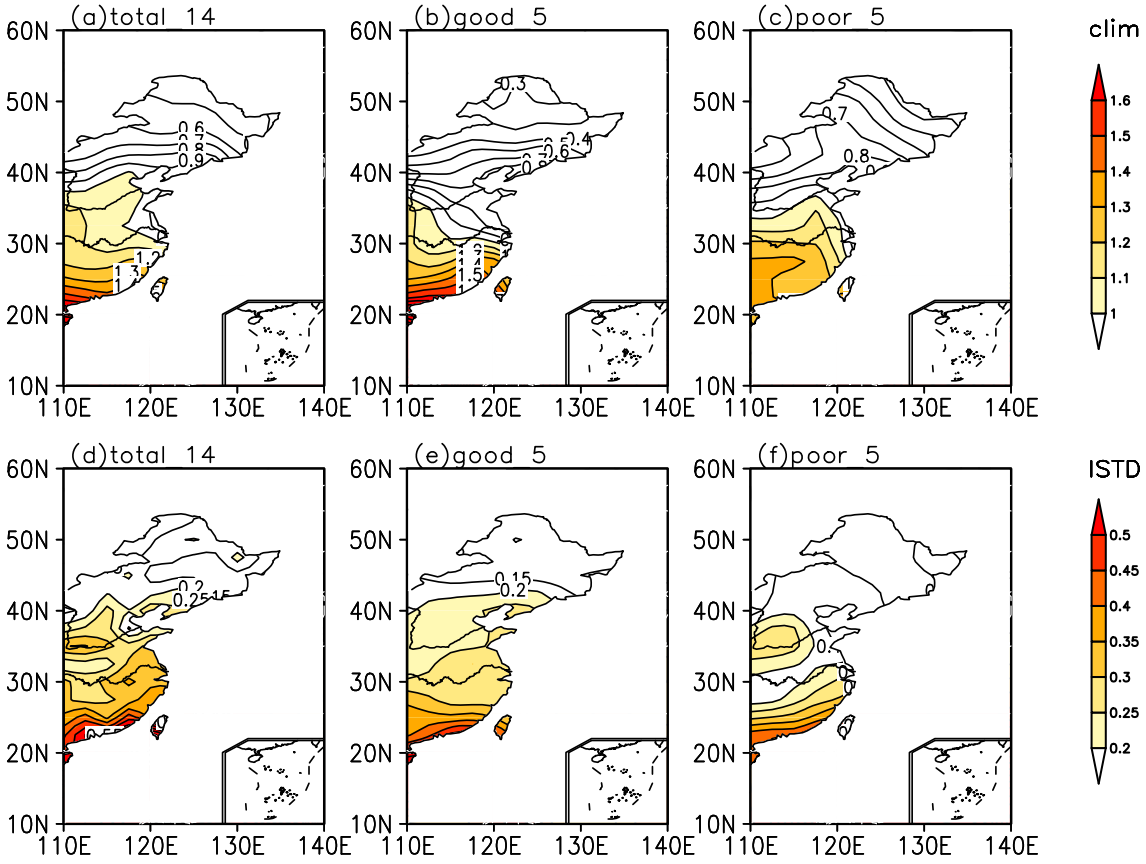

Figure 6. The model spread distribution of the (a,d) 14 CMIP5 models, (b,e) good models, and (c,f) poor models in climatology and ISTD of summer precipitation over Eastern China. (unit: mm day^{-1}).

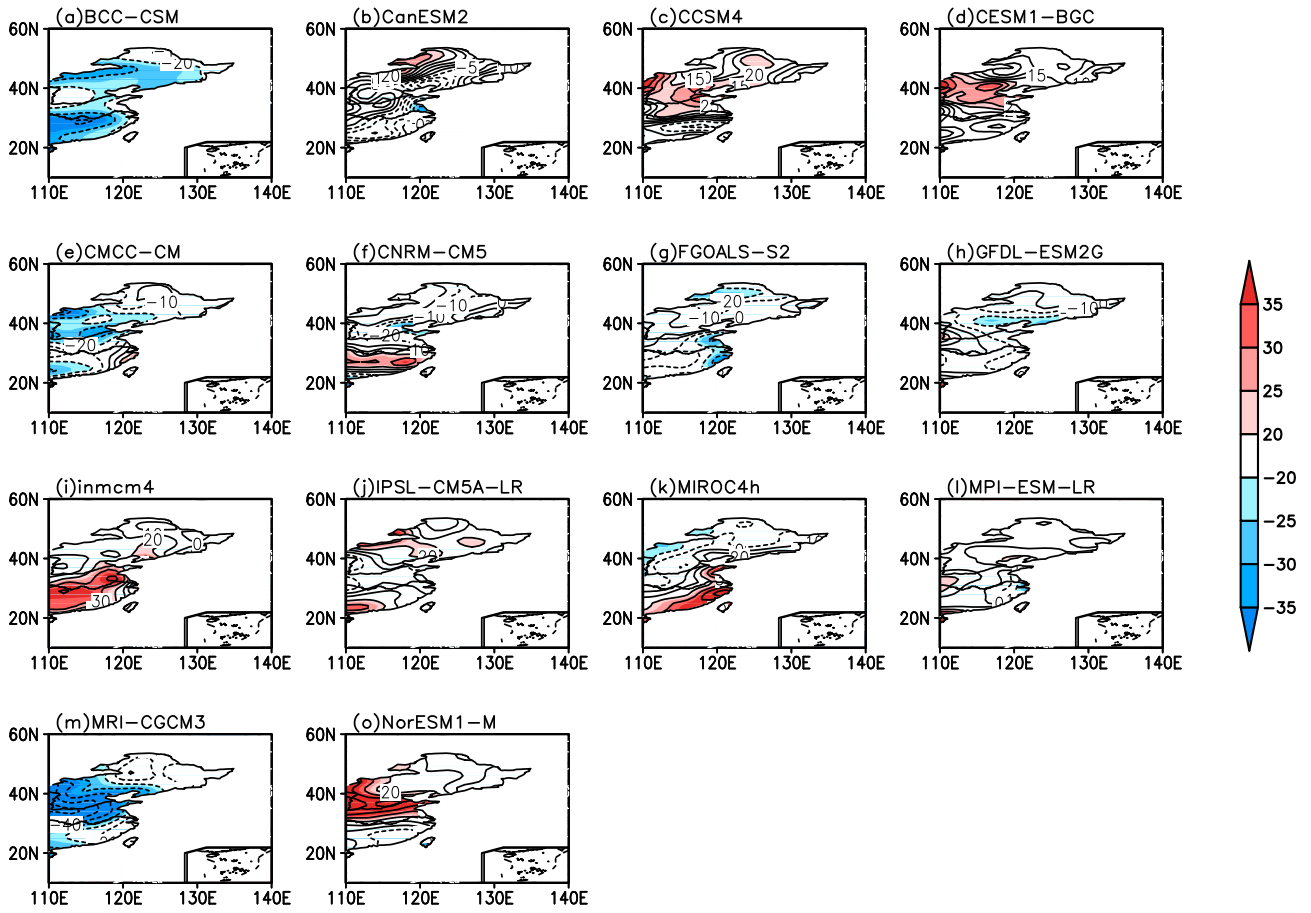

Figure 7. The ratios of the differences between individual model and AMME to AMME for climatological summer rainfall over Eastern China in 1979–2005. (unit: %).

1975; *Tao and Chen*, 1987; *Zhang et al*., 2006]. Thus, in the following, the uncertainties on simulated WPSH and EASWJ are analyzed.

[20] Figure 9 shows the zonal wind at 200 hPa in 14 CMIP5 models, along with the model spread for 1979–2005. Generally, two EASWJ cores are indicated in summer: Tibetan pattern (85°–100°E) and Iran pattern (45°–60°E) [*Kuang*, 2006]. The Tibetan pattern is closely related to the increase of summer rainfall over the lower reaches of Yangtze River and decrease over northern and southern China, while the Iran pattern is associated with the increased precipitation over northern and southern China and nonsignificant decreased precipitation over Yangtze River Basin. Large differences are indicated in the simulated EASWJ, in both intensity and location. Compared to the AMME, the CCSM4, CESM1-BGC, and NorESM1-M models overestimate the intensity of Tibetan pattern, which is closely associated with the overestimation of the simulated precipitation over lower reaches of Yangtze River. Although the simulated EASWJ of BCC-CSM and CMCC-CM models is much stronger than that of the AMME, the maximum center is not just over Tibetan Plateau, but extends to the coastal ocean, which provides the favorable environment for the precipitation increasing over coastal ocean but decreasing over Eastern China. Moreover, the model spread (Figure 9q) indicates large uncertainties along the dominant subtropical jets area and even extends to the coastal region. These large uncertainties on simulating intensity and location of EASWJ may affect the rainfall uncertainties over East Asia.

[21] Figure 10 shows geopotential height at 500 hPa in CMIP5 models, along with the model spread for 1979–2005. In comparison with the AMME (Figure 10p), WPSH strengthens and advances westward in CCSM4 and CESM1-BGC models, which may result in more precipitation over northern China shown in Figure 7. However, in CMCC-CM, FGOALS-S2, and MRI-CGCM3 models, the WPSH retreats eastward, which is associated with the negative precipitation biases. The MPI-ESM-LR model shows a similar pattern with the AMME, which is in agreement with the high reproducibility of precipitation. For model spread (Figure 10q), besides the obvious large center over northern Pacific, a small center locates in the main active regions of WPSH, indicating that most models can capture WPSH. But larger model spread locates near southern coastal area of China, where the westward advancing of WPSH is sensitive to pressure biases. Over all, the uncertainties in the simulated climatological summer precipitation over Eastern China are closely related to the uncertainties on simulating large-scale circulations (e.g., EASWJ and WPSH).

[22] Besides the uncertainties of climatology, large model spread is also indicated in the interannual variations. Eastern China is strongly under the influence of the East Asian

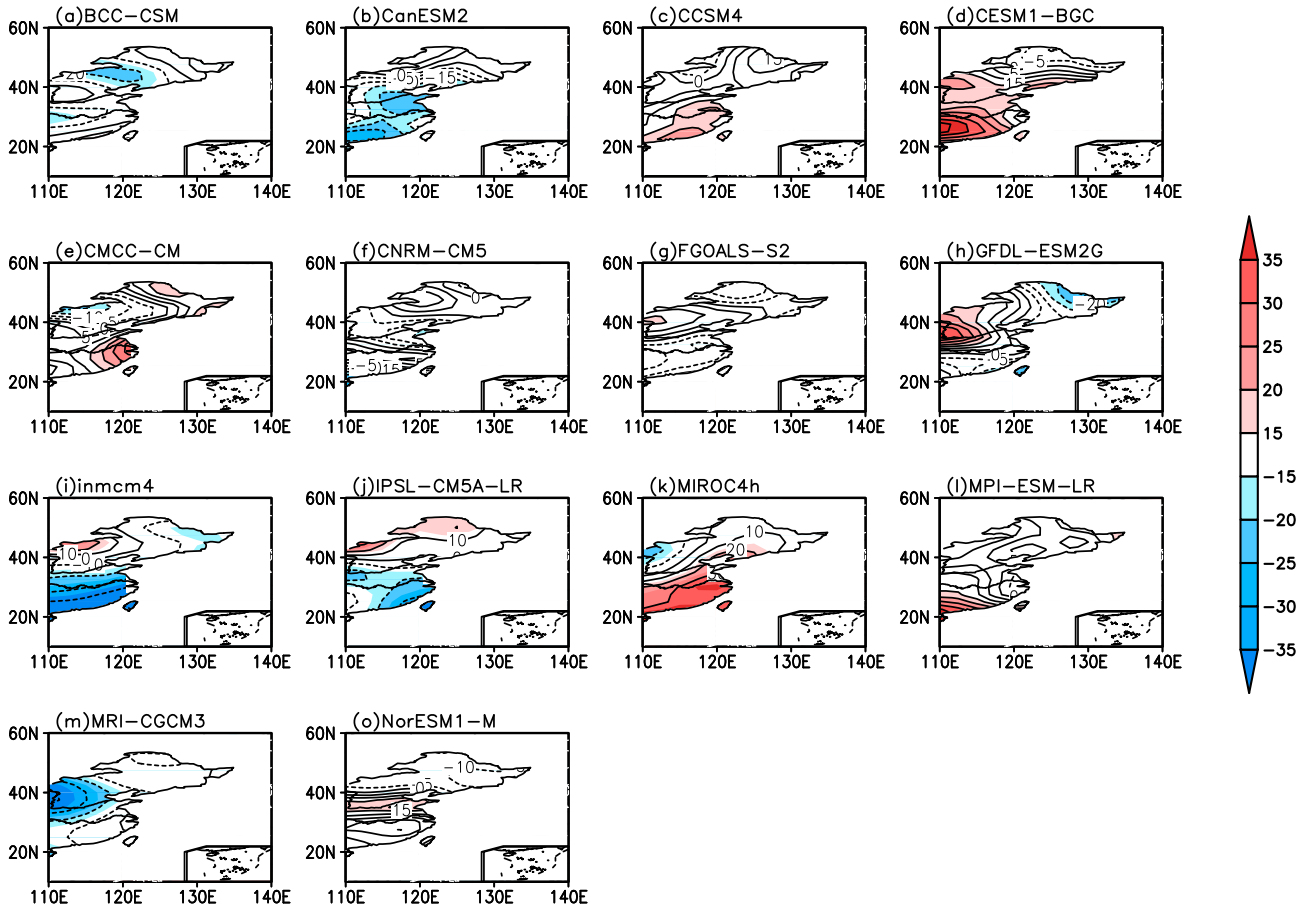

Figure 8. Same as Figure 7, but for ISTD. (unit: %).

Summer Monsoon (EASM) circulation through the moisture supply to East Asia. The interannual variation of summer precipitation over Eastern China is closely connected with the variation of EASM. To find the uncertainties on interannual variation of the simulated summer precipitation over Eastern China, the monsoon index is used to examine the EASM variations. In this study, we choose dynamical monsoon index defined by *Webster and Yang* [1992], which is calculated by the vertical shear of zonal winds between 850 hPa and 200 hPa averaged over area of 0°–20°N/40°–110°E (named as W-Y index). The W-Y index well depicts the variability of summer monsoon circulation over the broad tropical Asian regions [*Wang and Fan*, 1999; *Lau et al*., 2000]. Figure 11 shows the seasonal and annual evolution of the EASM for the CMIP5 models. Large uncertainties exist among the CMIP5 models, especially in summer (between the two blue dashed lines, with the W-Y index around −6 to 14 (Figure 11a). The bias of yearly W-Y index among CMIP5 models is around 16 to 24 (Figure 11b). Large yearly model spread exists from 1979 to 2005, with values around 2.9 to 5.34 (figure omitted). That suggests that large uncertainties in simulating interannual variation may also be related with the uncertainties in simulated EASM.

3.4. Uncertainties on the Regional Variability

[23] Since precipitation over the Eastern China has large spatial variations and the most sensitive region may be the southern China from above analysis, uncertainties for different subregions should be investigated. Figure 12 shows the annual cycle of the regional mean precipitation simulated by the 14 CMIP5 models in 1979–2005. Similar as the annual cycle of precipitation averaged over Eastern China (Figure 2), large uncertainties exist among the 14 models in summer. Meanwhile, another period with large uncertainties is from April to May in the YHRB (Figure 12b). It is in accordance with the evolution of rain belt as shown in Figure 3b, known as spring persistent rainfall [*Tian and Yasunari*, 1998; *Wan and Wu*, 2008]. In the subseasonal scale (summer, between the two blue dashed lines), larger uncertainties are found in the earlier summer in SC and YHRB, while in middle summer in NC and NEC. That is in accordance with daily model spread in summer (Figure 12e). For different regions, the model spread reaches the maximum in SC with the maximum value as 0.75, and minimum in NEC with the mean value around 0.18, suggesting that the most sensitive region is SC, which is quite in accordance with the result in section 3.2.

[24] Recently, many breaking-record heavy rainfall and prolonged drought events have been reported worldwide [*Field et al*., 2012]. Besides the daily evolution of total precipitation, the different-class precipitation variations are also important [*Zhu et al*., 2009; *Emori et al*., 2005; *Kimoto et al*., 2006], especially the nonrainfall, light, and heavy rainfall, which are related with the drought/flood disasters. Then,

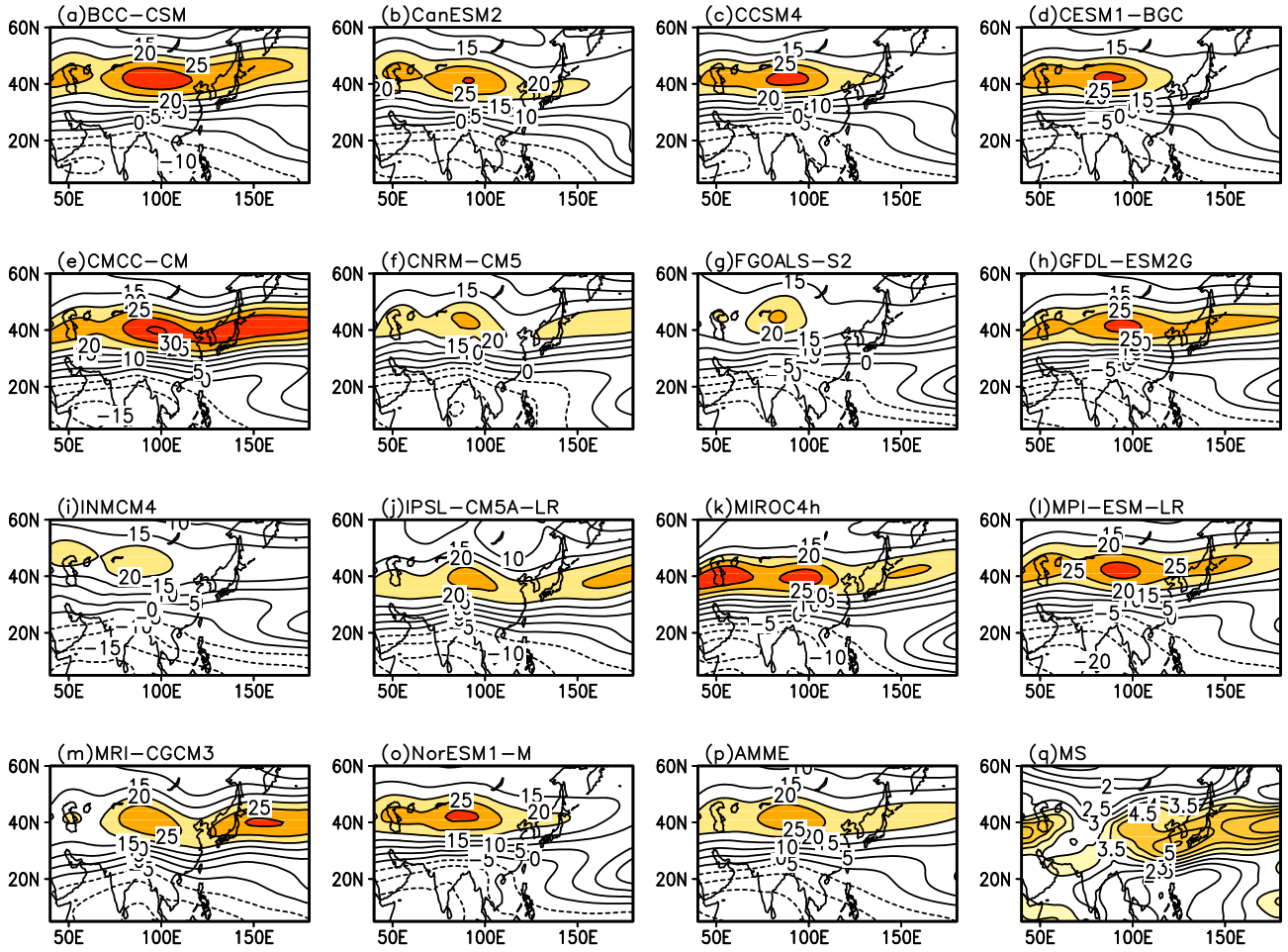

Figure 9. The summer mean zonal winds at 200 hPa in (a–o) 14 CMIP5 models, (p) AMME, and (q) model spread in 1979–2005. The shaded regions in Figures 9a–9p are with values over 20. (unit: m/s).

what are the uncertainties on the simulated different-class precipitation from the CMIP5 models?

[25] In this study, six classes of precipitation are chosen based on the daily summer precipitation intensity in 14 CMIP5 models, as nonrainfall (0–0.5 mm day^{-1}), very weak rainfall (0.5–5 mm day^{-1}), relatively weak rainfall (5–10 mm day^{-1}), moderate rainfall (10–20 mm day^{-1}), relatively heavy rainfall (20–35 mm day^{-1}), and very heavy rainfall (>35 mm day^{-1}). According to the four subregions, we calculate the frequency in different classes by daily summer precipitation.

[26] Figure 13 examines the histograms of precipitation frequency in the four subregions as a function of daily precipitation class. In the four subregions, the weak rainfall [0.5–10 mm day^{-1}] is the dominant rainfall in summer. Their frequencies do not differ much among 14 models, indicating small uncertainties in simulating weak rainfall. However, large uncertainties exist on the simulated frequency of nonrainfall and heavy rainfall [>20 mm day^{-1}]. Especially for the very heavy rainfall, as in SC, only six models can catch very heavy rainfalls but the other eight models do not. Similar results can be seen in the other three subregions. Moreover, as red bars in the figures, the AMME cannot well capture the heavy rainfall in four subregions and even misses all the very heavy rainfalls. Overall, larger uncertainties exist in the nonrainfall and heavy rainfall, suggesting that the MMEs may not be a better way to describe the flood and drought events than some individual models.

4. Conclusions and Discussions

[27] This study discusses the uncertainties on the simulated summer precipitation of 14 CMIP5 models over Eastern China, including climatology, interannual variation, regional variation, and different-class precipitation. Models with high S-index are selected as good models, and the GMME shows better performance than the AMME in both climatology and ISTD. However, model spreads do not differ much between the two MMEs. Thus, it is important to check uncertainty of individual model. The possible reason for the large model spread of precipitation lies in the uncertainties on simulating the large-scale circulations (both intensity and location), e.g., EASWJ, WPSH, and EASM. To estimate the regional variation, Eastern China is divided into four subregions. The annual cycle of regional simulated precipitation from the 14 CMIP5 models indicates that model uncertainties over Eastern China generally decrease from south to north, implying South China is the most sensitive region.

[28] Moreover, large uncertainties exist in the different-class precipitation. Most models can simulate the frequency of weak rainfall. However, few models can capture the very

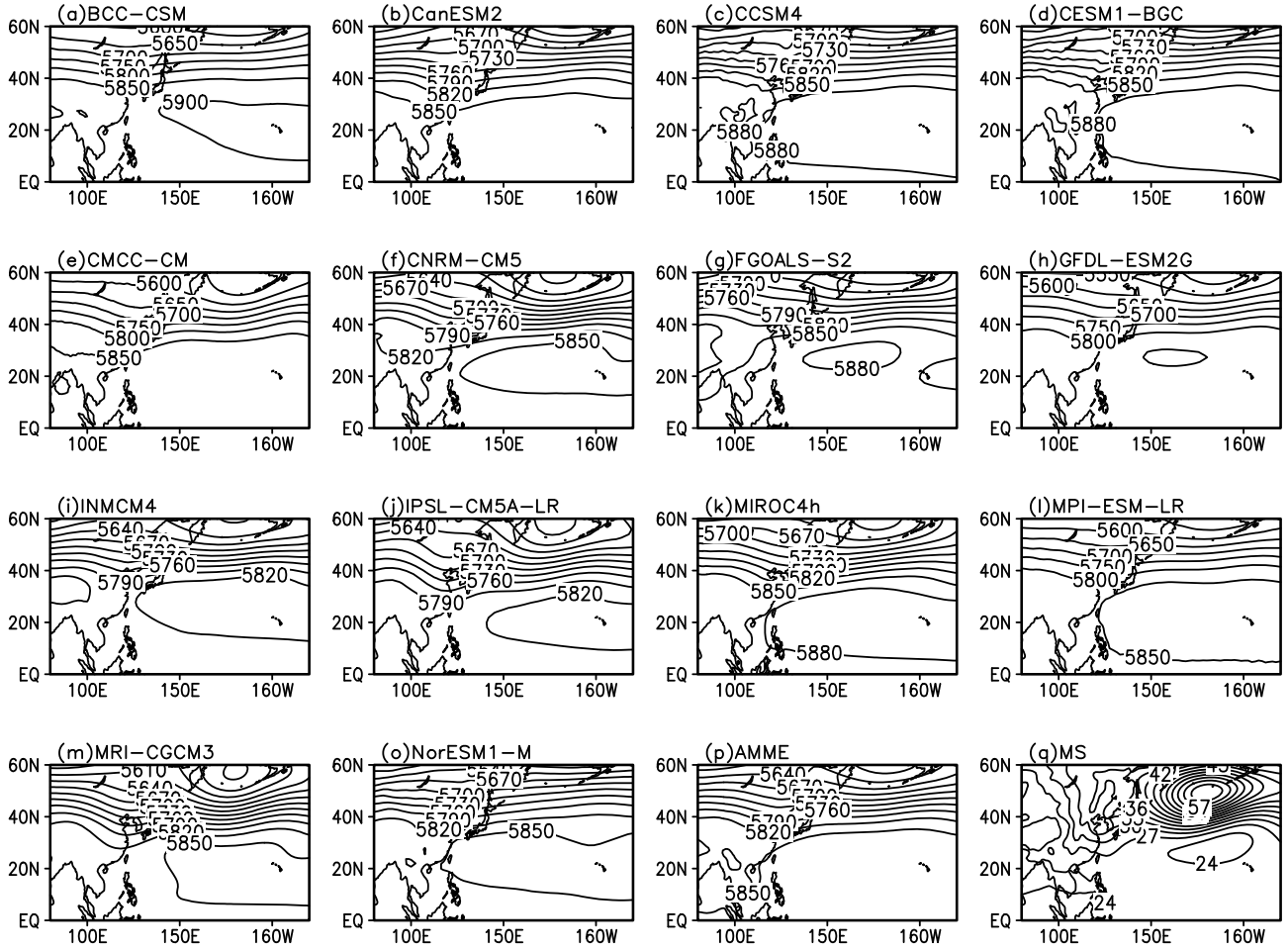

Figure 10. Same as Figure 9, but for geopotential height at 500 hPa. (unit: gpm).

heavy rainfall, indicating that large uncertainties exist on simulating heavy rainfall. Why do larger uncertainties exist in the description of different-class precipitation? One of the possible explanations is that the CMIP5 models may not well simulate different kinds of precipitation (e.g., cumulus convective precipitation, large-scale precipitation). Moreover, what kind of precipitation is dominant in different regions over Eastern China is not clear and the models play large uncertainties on simulating dominant kind of precipitation. Figure 14 shows the ratio of CCP to total precipitation in 14 CMIP5 models and the AMME. The ratios in Eastern China generally decrease from south to north, with maximum value in SC. In CNRM-CM5, FGOALS-S2, Inmcm4, and IPSL-CM5A-LR models, the dominant precipitation is CCP over almost entire Eastern China in summer, with the ratios higher than 80%. While in BCC-CSM, CMCC-CM, and MIROC4h models, the CCP is not the dominant rainfall. Thus, large uncertainties exist in the ratios of CCP to total precipitation. This is in agreement with previous studies, indicating that intermodel difference in CCP is generally larger than that in total and stratiform precipitation [*Xie et al*., 2005; *Song et al*., 2013]. These large uncertainties on the ratios may

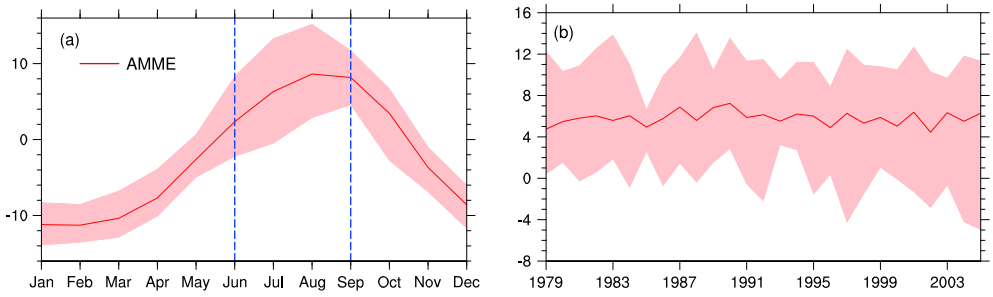

Figure 11. (a) Monthly variation and (b) yearly variation of W-Y index from AMME. The pink shading indicates the range of maximum and minimum W-Y index in 14 CMIP5 models. The blue dashed lines indicate summer time. (unit: m/s).

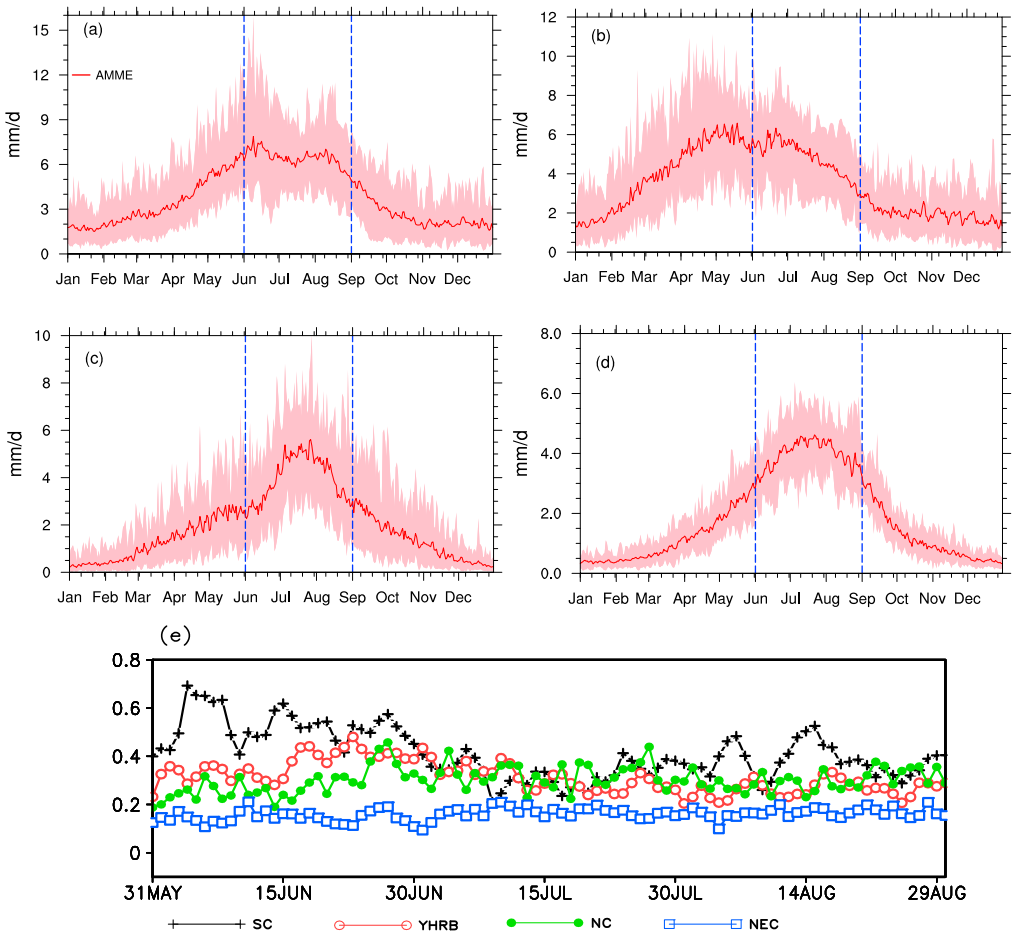

Figure 12. Annual cycle of AMME (red solid line) and range between maximum and minimum precipitation of the 14 CMIP5 models (pink shading) over (a) SC, (b) YHRB, (c) NC, and (d) NEC and the (e) daily model spread during summer time in four subregions in 1979–2005. The blue dashed lines indicate summer time. (unit: mm day^{-1}).

result in the large uncertainties on different-class precipitation. In models, different kinds of precipitation, namely cumulus convective precipitation and large-scale stratiform precipitation, are produced separately from the convection and microphysical parameterization schemes. These schemes may be quite different among models, which may lead to the large uncertainties on the ratios of the two kinds of precipitation. That suggests that different kinds of physical parameterizations should be used. *Huang et al.* [2009] suggested that the simulated precipitation over China was sensitive to different cumulus convection, radiative transfer, and land surface process parameterizations. *Emori et al.* [2005] discussed the sensitivity in the tails of the frequency distribution that is strongly influenced by physical parameterizations. Moreover, which physical parameterizations are superior for identifying the precipitation over Eastern China is not clear. In order to reduce these uncertainties, the physical process ensemble technique is one of the useful methods. Study of *Huang et al.* [2009] indicated that the physical process ensemble technique can obviously improve the performance of model in simulation of summer precipitation over Eastern China.

[29] The other possible reason may be the model resolution. *Kimoto* [2005] compared high and medium resolution versions for the present-day climate over Eastern China. The results indicated that the higher resolution version better represents the frequency distribution of different-class precipitation, which was also confirmed by *Zhu et al.* [2009]. *Kusunoki et al.* [2006] showed that, unlike lower-resolution models, atmospheric general circulation model with 20 km grid size reproduced a realistic Baiu rain band in June and July under present-day climate conditions in terms of the geographical distribution and northward season march. Moreover, is the spatial resolution the higher the better? *Chan et al.* [2012] compared different spatial resolutions (50, 12, and 1.5 km) of a regional climate model for simulating daily precipitation extremes over southern United Kingdom without convective parameterization. The results indicated that in general, there were some improvements when model resolution was increased from 50 km to 12 km, but no further clear improvements from 12 km to 1.5 km. These indicate the increasing resolution does not necessarily lead to the improvement on the simulation of summer precipitation. Thus, suitable resolution is also an important element in simulating heavy rainfall over Eastern China. In order to clearly confirm this speculation, some experiments that change the resolution but using the same convection and relevant physics should be examined in the future.

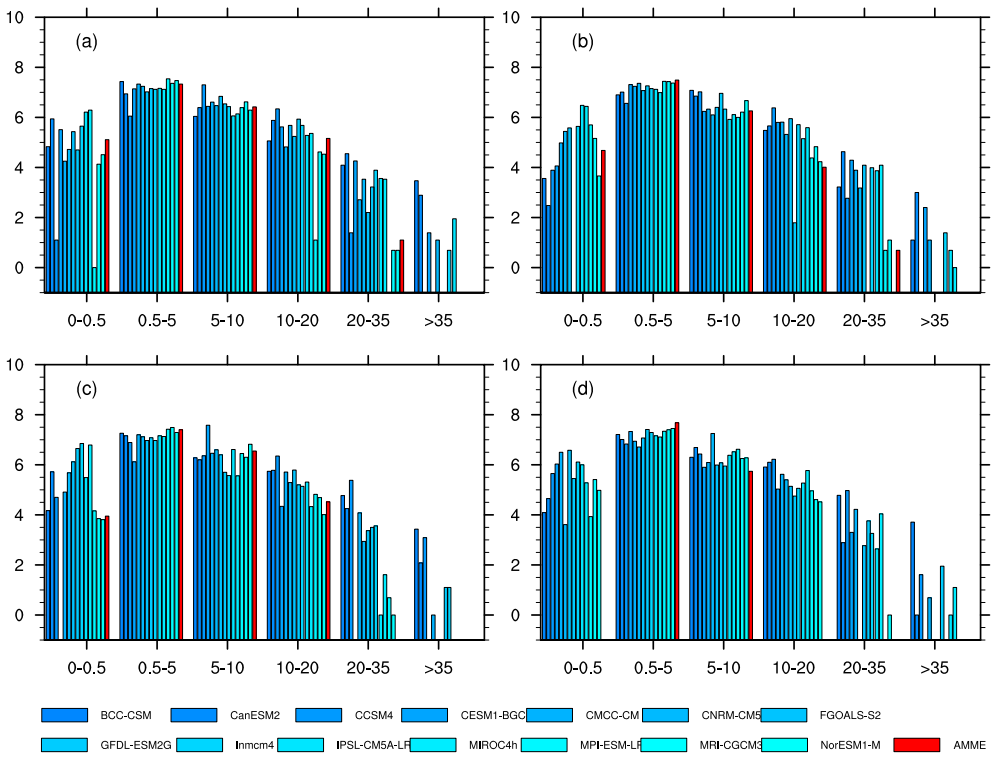

Figure 13. Histogram of frequency of the simulated different-class precipitation from 14 CMIP5 models and AMME in the four subregions of Eastern China: (a) SC, (b) YHRB, (c) NC, and (d) NEC. The ordinate is logarithm of relative frequency.

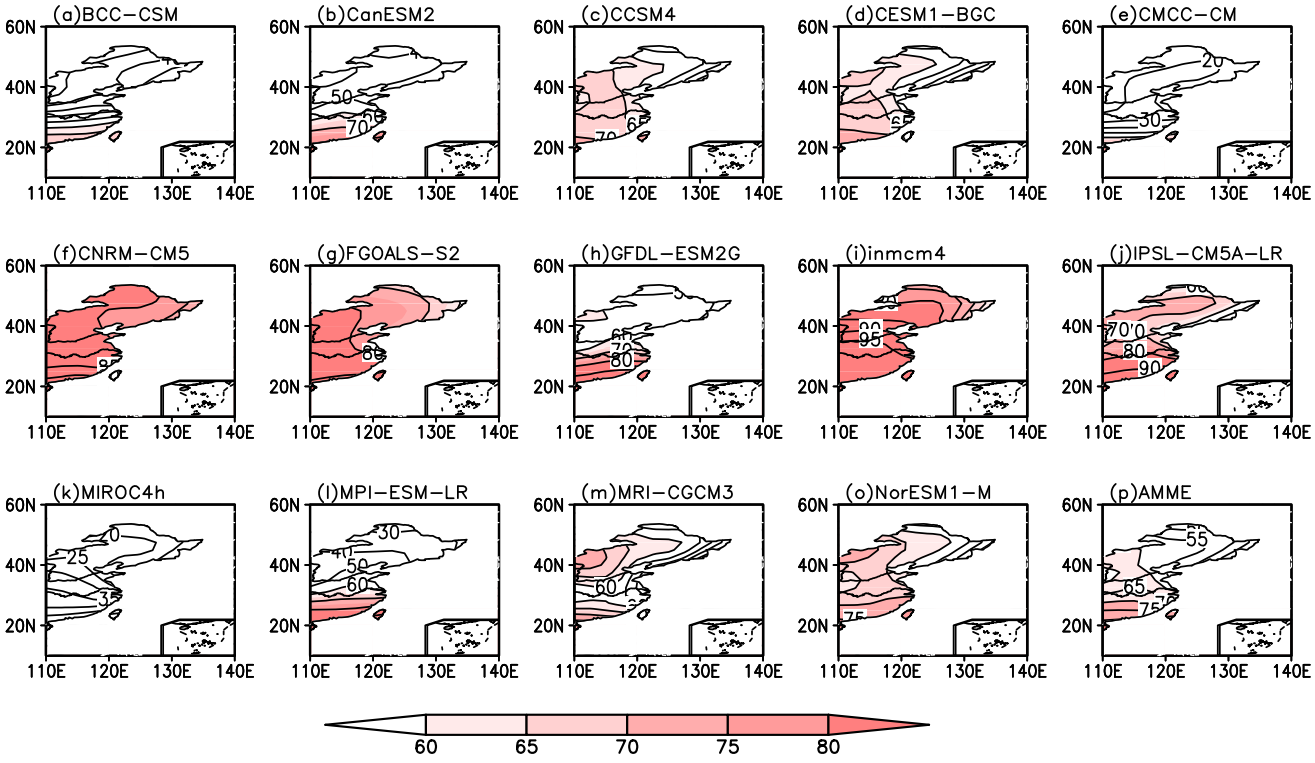

Figure 14. The ratio of cumulus convective precipitation to total precipitation over Eastern China in 1979–2005 from 14 CMIP5 models and AMME. (unit: %).

[30] **Acknowledgments.** We thank the editor and three anonymous reviewers for their valuable comments and suggestions. This study is jointly sponsored by National Natural Science Foundation of China (Grant Nos. 41105044, 41205038 and 41130963), the National Basic Research Program of China (973 Program; grant no. 2012CB955901), Major Program of National Natural Science Foundation of China (No.51190090), and the National Basic Research Program of China (973 Program; grant no. 2011CB952002).

References

Akiyama, T. (1975), Southerly transversal moisture flux into the extremely heavy rainfall zone in the Baiu season, *J. Meteor. Soc. Jpn.*, *53*, 304–316.

Belleflamme, A., X. Fettweis, C. Lang, and M. Erpicum (2012), Current and future atmospheric circulation at 500 hPa over Greenland simulated by the CMIP3 and CMIP5 global models, *Clim. Dynam.*, doi:10.1007/s00382-012-1538-2.

Chan, S. C., E. J. Kendon, H. J. Fowler, S. Blenkinsop, C. A. T. Ferro, and D. B. Stephenson (2012), Does increasing the spatial resolution of a regional climate model improve the simulated daily precipitation in a regional climate model?, *Clim. Dynam.*, doi:10.1007/s00382-012-1568-9.

Chen, H. S., S. Shi, and J. Zhou (2011), Evaluation of recent 50 years extreme climate events over China simulated by Beijing Climate Center (BCC) climate model, *Trans. Atmos. Sci.*, *34*(5), 513–528.

Chen, L., Y. Q. Yu, and D. Z. Sun (2013), Cloud and water vapor feedbacks to the El Nino warming: Are they still biased in CMIP5 models?, *J. Climate*, *26*, 4,947–4,961.

Christensen, J. H., et al. (2007), Regional climate projections, in *Climate Change 2007: The Physical Science Basis. Contribution of Working Group I to the Fourth Assessment Report of the Intergovernmental Panel on Climate Change*, edited by S. Solomon et al., Cambridge Univ. Press, Cambridge.

Cubasch, U., G. A. Meehl, G. J. Boer, R. J. Stouffer, M. Dix, A. Noda, C. A. Senior, S. Raper, and K. S. Yap (2001), Projections of future climate change, in *Climate Change 2001: The Scientific Basis. Contribution of Working Group I to the Third Assessment Report of the Intergovernmental Panel on Climate Change*, edited by J. T. Houghton et al., pp. 525–582, Cambridge Univ. Press, Cambridge.

Ding, Y., and J. C. L. Chan (2005), The East Asian summer monsoons: An overview, *Meteorol. Atmos. Phys.*, *89*, 117–142, doi:10.1007/s00703-005-0125-z.

Emori, S., A. Hasegawa, T. Suzuki, and K. Dairaku (2005), Validation, parameterization dependence and future projection of daily precipitation simulated with a high resolution atmospheric GCM, *Geophys. Res. Lett.*, *32*, L06708, doi:10.1029/2004GL022306.

Field, C. B., et al. Eds. (2012), Managing the Risks of Extreme Events and Disasters to Advance Climate Change Adaptation: Special Report of the Intergovernmental Panel on Climate Change. http://ipcc-wg2.gov/SREX/.

Hawkins, E., and R. Sutton (2009), The potential to narrow uncertainty in regional climate predictions, *Bull. Am. Meteorol. Soc.*, *90*, 1095, doi:10.1175/2009BAMS2607.1.

Hirota, N., and Y. N. Takayabu (2013), Reproducibility of precipitation distribution over the tropical oceans in CMIP5 multi-climate models compared to CMIP3, *Clim. Dynam.*, doi:10.1007/s00382-013-1839-0.

Hirota, N., Y. N. Takayabu, M. Watanabe, and M. Kimoto (2011), Precipitation reproducibility over tropical oceans and its relationship to the double ITCZ problem in CMIP3 and MIROC5 climate models, *J. Climate*, *24*, 4859–4873.

Hu, Z. Z., M. Latif, E. Roeckner, and L. Bengtsson (2000), Intensified Asian summer monsoon and its variability in a coupled model forced by increasing greenhouse gas concentrations, *Geophys. Res. Lett.*, *27*, 2681–2684.

Huang, R., J. Chen, and G. Huang (2007), Characteristics and variations of the East Asian monsoon system and its impacts on climate disasters in China, *Adv. Atmos. Sci.*, *24*, 993–1023.

Huang, A. N., Y. C. Zhang, and J. Zhu (2009), Effects of the physical process ensemble technique on simulation of summer precipitation over China, *Acta Meteorol. Sin.*, *23*(6), 713–724.

Huang, D. Q., M. Takahashi, and Y. C. Zhang (2011), Analysis of the Baiu precipitation and associated circulations simulated by the MIROC coupled climate system model, *J. Meteor. Soc. Jpn.*, *89*(6), 625–636.

Jiang, Z. H., T. T. Ma, and Z. W. Wu (2012), China coldwave duration in a warming winter: Change of the leading mode, *Theor. Appl. Climatol.*, *110*, 65–75.

Jones, C., and L. Carvalho (2013), Climate change in the South American Monsoon System: present climate and CMIP5 projections, *J. Climate*, doi:10.1175/JCLI-D-12-00412.1, in press.

Kimoto, M. (2005), Simulated change of the east Asian circulation under the global warming scenario, *Geophys. Res. Lett.*, *32*, L16701, doi:10.1029/2005GL023383.

Kimoto, M., N. Yasutomi, C. Yokoyama, N. Yasutomi, C. Yokoyama, and S. Emori (2006), Projected changes in precipitation characteristics around Japan under the global warming, *Sola*, *1*, 85–88.

Knutti, R. (2010), The end of model democracy?, *Clim. Change*, *102*, 395–404.

Krishnamurti, T. N., C. M. Kishtawal, Z. Zhang, T. Larow, D. Bachiochi, and E. Willford (2000), Multimodel ensemble forecasts for weather and seasonal climate, *J. Climate*, *13*, 4196–4216.

Kuang, X. Y. (2006), Study on the seasonal and interannual variations of the East Asian subtropical westerly jet and its thermal mechanism and climate effects, Ph.D. dissertation, Nanjing University, PP159.

Kusunoki, S., J. Yoshimura, H. Yoshimura, A. Noda, K. Oouchi, and R. Mizuta (2006), Change of Baiu rain band in global warming projection by an atmospheric general circulation model with 20-km grid size, *J. Meteor. Soc. Jpn.*, *84*, 581–611.

Lau, K. M., K. M. Kim, and S. Yang (2000), Dynamical and boundary forcing characteristics of regional components of the Asian summer monsoon, *J. Climate*, *13*, 2461–2482.

Lau, W. K.-M., H.-T. Wu, and K. M. Kim (2013), A canonical response of precipitation characteristics to global warming from CMIP5 models, *Geophys. Res. Lett.*, *40*, 3163–3169, doi:10.1002/grl.50420.

Lee, J. Y., and B. Wang (2012), Future change of global monsoon in the CMIP5, *Clim. Dynam.*, doi:10.1007/s00382-012-1564-0.

Li, B., and T. J. Zhou (2010), Projected climate change over China under SRES A1B scenario: Multi-model ensemble and uncertainties (in Chinese), *Adv. Clim. Change Res.*, *6*(4), 270–276.

Lu, R., and Y. Fu (2009), Intensification of East Asian summer rainfall interannual variability in the twenty-first century simulated by 12 CMIP3 coupled models, *J. Climate*, doi:10.1175/2009JCLI3130.1.

Lu, R., Y. Li, and B. Dong (2007), East Asian precipitation increase under the global warming, *J. Korean. Meteor. Soc.*, *43*(3), 267–272.

Meehl, G. A., et al. (2007a), Global climate projections, in *Climate Change 2007: The Physical Science Basis*, edited by M. Allen and G. Ballabh Pant, pp. 747–845, Cambridge Univ. Press, Cambridge, UK and New York.

Meehl, G. A., et al. (2007b), Global climate projections, in *Climate Change 2007: The Physical Science Basis. Contribution of Working Group I to the Fourth Assessment Report of the Intergovernmental Panel on Climate Change*, edited by S. Solomon et al., Cambridge Univ. Press, Cambridge.

Min, S. K., E. H. Park, and W. T. Kwon (2004), Future projections of East Asian climate change from multi-AOGCM ensembles of IPCC SRES scenario simulations, *J. Meteor. Soc. Jpn.*, *82*, 1187–1211.

Mizuta, R. (2012), Intensification of extratropical cyclones associated with the polar jet change in the CMIP5 global warming projections, *Geophys. Res. Lett.*, *39*, L19707, doi:10.1029/2012GL053032.

Randall, D. A., et al. (2007), *Climate Models and Their Evaluation*, pp. 589–662, Cambridge Univ. Press, Cambridge, UK.

Scheff, J., and D. M. W. Frierson (2012), Robust future precipitation declines in CMIP5 largely reflect the poleward expansion of model subtropical dry zones, *Geophys. Res. Lett.*, *39*, L18704, doi:10.1029/2012GL052910.

Seo, K., and J. Ok (2013), Assessing future changes in the East Asian summer monsoon using CMIP3 models: Results from the best model ensemble, *J. Climate*, *26*, 1807–1817.

Song, H., W. Lin, Y. Lin, A. Wolf, R. Neggers, L. Donner, A. Del Geino, and Y. Liu (2013), Evaluation of precipitation simulated by seven SCMs against the ARM observation at the SGP site, *J. Climate*, *26*, 5,467–5,492.

Stephens, G. L. (2005), Cloud feedbacks in the climate system: A critical review, *J. Climate*, *18*(2), 237–273.

Sun, Y., and Y. H. Ding (2008), An assessment on the performance of IPCC AR4 climate models in simulating interdecadal variations of the East Asian summer monsoon, *Acta Meteorol. Sin.*, *22*(4), 472–488.

Tao, S. Y., and L. X. Chen (1987), A review of recent research on the East Asian summer monsoon in China, in *Monsoon Meteorology*, edited by C. P. Chang and T. N. Krishnamurti, pp. 60–92, Oxford Univ. Press, London.

Taylor, K. E. (2001), Summarizing multiple aspects of model performance in a single diagram, *J. Geophys. Res.*, *106*, 7183–7192.

Taylor, K. E., R. J. Stouffer, and G. A. Meehl (2012), An overview of CMIP5 and the experiment design, *Bull. Am. Meteorol. Soc.*, *93*, 485–498, doi:10.1175/BAMS-D-11-00094.1.

Tebaldi, C., and R. Knutti (2007), The use of the multi-model ensemble in probabilistic climate projections, *Phil. Trans. Roy. Soc. A.*, *365*, 2,053–2,075.

Tian, S. F., and T. Yasunari (1998), Climatological aspects and mechanism of Spring Persistent Rains over central China, *J. Meteorol. Soc. Jpn.*, *76*, 57–71.

Wan, R. J., and G. X. Wu (2008), Temporal and spatial distribution of the spring persistent rains over southeastern China (in Chinese), *Acta Meteorol. Sin.*, *66*, 310–319.

Wang, B., and Z. Fan (1999), Choice of South Asian summer monsoon indices, *Bull. Am. Meteorol. Soc.*, *80*, 629–638.

Webster, P. J., and S. Yang (1992), Monsoon and ENSO: Selectively interactive systems, *Q. J. Roy. Meteor. Soc.*, *118*, 877–926.

Xie, S. C., M. H. Zhang, and M. Branson (2005), Simulations of midlatitude frontal clouds by single-column and cloud-resolving models during

theAtmospheric Radiation Measurement March 2000 cloud intensive operational period, *J. Geophys. Res.*, *110*, DI5S03, doi:10.1029/2004JD005119.

Ye, H., and R. Lu (2012), Dominant patterns of summer rainfall anomalies in East China during 1951-2006, *Adv. Atmos. Sci.*, *29*, 695–704.

Zhang, Y. C., X. Y. Kuang, W. D. Guo, and T. J. Zhou (2006), Seasonal evolution of the upper-tropospheric westerly jet core over East Asia, *Geophys. Res. Lett.*, *33*, L11708, doi:10.1029/2006GL026377.

Zhou, T., and R. Yu (2006), Twentieth century surface air temperature over China and the globe simulated by coupled climate models, *J. Climate*, *19*(22), 5843–5858.

Zhou, T. J., L. J. Li, H. M. Li, and Q. Bao (2008), Progress in climate change attribution and projection studies (in Chinese), *Chin. J. Atmos. Sci.*, *32*(4), 906–922.

Zhu, J., Y. C. Zhang, and D. Q. Huang (2009), Analysis of changes in different-class precipitation over Eastern China under global warming (in Chinese), *Plateau Meteorol.*, *28*(4), 889–896.